Review

Composite two-particle sources[*]

Michael Moskalets[1,a], Janne Kotilahti[2], Pablo Burset[2], and Christian Flindt[2]

[1] Department of Metal and Semiconductor Physics, NTU Kharkiv Polytechnic Institute, 61002 Kharkiv, Ukraine
[2] Department of Applied Physics, Aalto University, 00076 Aalto, Finland

Abstract. Multi-particle sources constitute an interesting new paradigm following the recent development of on-demand single-electron sources. Versatile devices can be designed using several single-electron sources, possibly of different types, coupled to the same quantum circuit. However, if combined *non-locally* to avoid cross-talk, the resulting architecture becomes very sensitive to electronic decoherence. To circumvent this problem, we here analyse two-particle sources that operate with several single-electron (or hole) emitters attached in series to the same electronic waveguide. Using Floquet scattering theory we demonstrate how such a device can emit exactly two electrons without exciting unwanted electron-hole pairs if the driving is adiabatic. Going beyond the adiabatic regime, perfect two-electron emission can be achieved by driving two quantum dot levels across the Fermi level of the external reservoir. If a single-electron source is combined with a source of holes, the emitted particles can annihilate each other in a process which is governed by the overlap of their wave functions. Importantly, the degree of annihilation can be controlled by tuning the emission times, and the overlap can be determined by measuring the shot noise after a beam splitter. In contrast to a Hong-Ou-Mandel experiment, the wave functions overlap close to the emitters and not after propagating to the beam splitter, making the shot noise reduction less susceptible to electronic decoherence.

1 Introduction

On-demand single-electron sources [1–4] make it possible to perform quantum optics experiments with electrons, and they form the basis of the rapidly developing field of *quantum coherent electronics* [5,6]. Electronic counterparts of the famous Hanbury-Brown and Twiss effect [7–14] and Hong-Ou-Mandel interference [8,15–20] have already been demonstrated experimentally. Quantum tomography of single-electron states has also been proposed and realized [21–24]. However, one challenging issue working with electrons is decoherence and relaxation caused by neighboring electrons in the waveguides, which can significantly degrade quantum effects, resulting

---
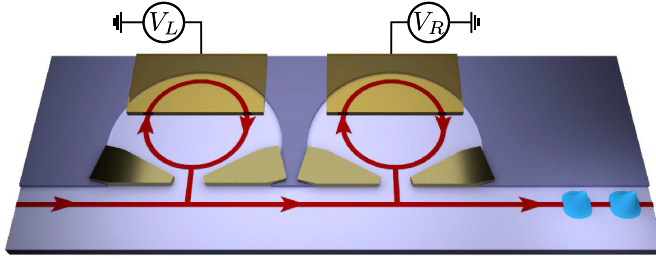
Fig. 1. A composite two-electron source can be constructed from single-electron sources located side by side. Here, two quantum capacitors in series are driven by separate gate voltages. Each capacitor is formed by a circular edge state (in red) and a metallic top gate. Electrons (in blue) are emitted into an edge state in the direction indicated by arrows.

for example in a non-perfect Pauli dip in the shot noise (the fermionic analogue of the Hong-Ou-Mandel peak in quantum optics) [17]. Several methods are currently being developed to prevent decoherence, including quantum environment engineering [25–29], and the emission of electrons high above the Fermi level [24,30,31]. Still, recent experimental results on energy relaxation indicate that the longest mean free path is achieved by emitting the electrons close to the Fermi level [28]. For quantum information processing, it may thus be favorable to use single-electron sources that emit particles right on top of the Fermi sea, for instance, a quantum capacitor [32–35], a leviton source [8,36–38], or the recently proposed emitter based on time-dependent local gating [39].

While single-electron emitters have been investigated both experimentally and theoretically, much less is known about more complex devices such as multi-particle sources, although some experimental progress in this direction has already been reported [8,40–44]. In this work, we analyze two-electron sources consisting of several single-electron sources connected in series as illustrated in Figure 1 [45]. Here we show two quantum capacitors attached to the same edge state, but one may also consider combinations of different types of emitters, for example by integrating a quantum capacitor [32] with a source of levitons [8]. Importantly, as we will discuss in detail, one can combine a single-electron emitter with a source of holes [16], which will enable the controlled creation of superpositions of quantum states which have different numbers of fermions. Note also that Coulomb interactions can presumably affect the emission process itself [46,47], which has yet to be confirmed experimentally. Here, we do not take this effect into account.

The rest of the paper is organized as follows: in Section 2, we provide a brief account of the excess correlation function formalism and demonstrate its usefulness for the analysis of single and few-particle emitters. In Section 3, we outline the theory of composite two-electron sources based on the scattering properties of the individual single-particle emitters. We provide several examples of composite two-particle emitters in Section 4, and show that it is possible to emit exactly two electrons without exciting unwanted electron-hole pairs if the driving is adiabatic. In a specific case, perfect two-electron emission can also be achieved in the non-adiabatic regime. Technical details of our calculations are deferred to the Supplementary Material.

2 Excess correlation function

The first-order correlation function is defined as $\mathcal{G}^{(1)}(1;2) = \langle \hat{\Psi}^{\dagger}(1)\hat{\Psi}(2) \rangle$, where $\hat{\Psi}$ in our case is the field operator of electrons in the conductor of interest, and the

brackets $\langle \ldots \rangle$ denote the quantum-statistical average. The correlation function can be calculated using any many-body formalism, and in Section 3 we show in particular how it can be evaluated using scattering theory.

The correlation function $\mathcal{G}^{(1)}$ is additive in the number of electrons, which makes it a useful theoretical tool to characterize the excitations emitted by a source into a conductor. We just need to calculate $\mathcal{G}^{(1)}$ with the source turned on and off and evaluate the difference known as *the excess first-order correlation function* [21,48,49]

$$G^{(1)}(1;2) = \mathcal{G}^{(1)}_{\text{on}}(1;2) - \mathcal{G}^{(1)}_{\text{off}}(1;2). \tag{1}$$

To be specific, we consider a chiral one-dimensional conductor and fix the spatial coordinates at an arbitrary position downstream from the source, $x_1^{(0)} = x_2^{(0)} = x_D$, keeping only the times t_1 and t_2. For a linear (or linearized) dispersion relation, $E - \mu = v_\mu (p - p_\mu)$, the correlation function at different coordinates can be calculated using the substitution, $t_j \to t_j - v_\mu (x_j - x_D)$, with $j = 1, 2$, where μ is the Fermi energy of the electrons in the conductor and $v_\mu (p_\mu)$ is the velocity (momentum) of electrons at energy $E = \mu$. We restrict ourselves to non-interacting electrons, where $G^{(1)}$ provides complete information about the injected particles, and we set the temperature to zero to keep the discussion simple. For the purposes of this work, we consider only the regimes of perfect injection, where a controlled number of particles are injected without exciting unwanted electron-hole pairs.

2.1 Single-particle emission

If the source emits a single particle, the excess first-order correlation function reads [50]

$$G^{(1)}(t_1;t_2) = \eta \frac{e^{\frac{i}{\hbar}\mu(t_1-t_2)}}{v_\mu} \psi^*(t_1) \psi(t_2), \tag{2}$$

where $\eta = +1$ stands for the injection of an electron and $\eta = -1$ for a hole.

The wave function is normalized such that

$$\int dt \, |\psi(t)|^2 = 1, \tag{3}$$

having introduced the factor of $1/v_\mu$ in equation (2), so that we can formulate the normalization condition as an integral over time, instead of over space. It turns out to be convenient to introduce the formal factor $e^{\frac{i}{\hbar}\mu(t_1-t_2)}$ to describe the injection of an electron on top of the Fermi sea of the conductor, for example for a leviton source [51].

The correlation function is idempotent in the sense that

$$\int dt G^{(1)}(t_1;t) G^{(1)}(t;t_2) = \frac{\eta}{v_\mu} G^{(1)}(t_1;t_2), \tag{4}$$

which is characteristic for a pure state. A discussion of single-particle emission at non-zero temperatures, where the injected state is mixed rather than pure, can be found in references [52–54].

2.2 Two-particle emission

For a source that emits two particles, we have [50]

$$G^{(1)}(t_1; t_2) = \frac{e^{\frac{i}{\hbar}\mu(t_1 - t_2)}}{v_\mu} \sum_{\alpha=1}^{2} \eta_\alpha \psi_\alpha^*(t_1) \psi_\alpha(t_2).$$ (5)

If the source injects two particles of the same kind, two electrons or two holes, we have $\eta_1 \eta_2 = +1$, and the corresponding wave functions are orthogonal to each other, meaning that their overlap integral

$$J = \int dt \psi_1^*(t) \psi_2(t),$$ (6)

vanishes, $J_+ = 0$ (here the subscript denotes the product sign $\eta_1 \eta_2$). This fact is the manifestation of the Pauli exclusion principle for fermions injected into the same quantum channel, see e.g. reference [55].

By contrast, if the two-particle source emits one electron and one hole, $\eta_1 \eta_2 = -1$, the overlap integral is not necessarily zero, $J_- \neq 0$. To clarify the physics behind this observation, we need to analyse the two-particle wave function.

2.3 Electron-hole emission and annihilation

The fermionic two-particle wave function is represented by the following Slater determinant containing the single-particle wave functions, ψ_α,

$$\psi^{(2)}(t_1; t_2) = \begin{vmatrix} \psi_1(t_1) & \psi_2(t_1) \\ \psi_1(t_2) & \psi_2(t_2) \end{vmatrix}.$$ (7)

The integral of the squared wave function gives us the number of injected particles,

$$N = \iint dt_1 dt_2 \left| \psi^{(2)}(t_1; t_2) \right|^2 = 2 \left(1 - |J|^2\right),$$ (8)

having used the normalization of the single-particle wave functions according to equation (3) together with the definition of the overlap integral in equation (6).

Note that in the case of electron-hole injection, simply using $G^{(1)}$ for calculating the number of particles is incorrect, since $\int dt G^{(1)}(t; t)$ gives us the difference, not the sum of the number of injected particles.

If two particles of the same kind are injected, their wave functions are orthogonal, $J_+ = 0$, and the number of injected particles is $N_+ = 2$, as expected. The injected state $|\psi^{(2)}\rangle$ is a two-particle state, $|\psi^{(2)}\rangle = |ee\rangle$ or $|\psi^{(2)}\rangle = |hh\rangle$, where e stands for an electron and h stands for a hole.

If an electron and a hole are injected, their wave functions are not orthogonal, $J_- \neq 0$, and the number of injected particles is less than expected, $N_- < 2$, according to equation (8). One can interpret this suppression as being caused by the two injected particles annihilating each other with a probability given by the squared overlap integral, $|J_-|^2$. One may think of the electron emitted by one source as being reabsorbed by the other source which emits a hole (or *vice versa*) [45,56–58]. As such,
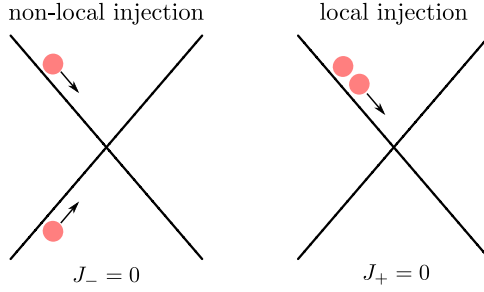
Fig. 2. Non-local and local injection of fermions on a beam splitter. Left panel: if particles are injected into different input arms, the overlap integral in equation (6) describes the scattering on the beam splitter, subject to the Pauli exclusion principle for electron-electron or hole-hole interference, $J_+ \neq 0$, but not for the simultaneous arrival of an electron and a hole, $J_- = 0$. Right panel: if two particles are injected into the same input arm, the overlap integral rather characterizes the injection process. The Pauli exclusion principle demands that the overlap vanishes, $J_+ = 0$, if two electrons or two holes are injected. Otherwise, $J_- \neq 0$ is the amplitude for the particles to annihilate each other according to equation (9).

the emitted state is a coherent superposition of the two-particle electron-hole state, $|eh\rangle$, and the state without any injected particles, the vacuum state $|0\rangle$,

$$|\psi^{(2)}\rangle = \sqrt{1 - |J_-|^2}\,|eh\rangle + J_-\,|0\rangle. \tag{9}$$

As we now go on to show, the number of injected particles in equation (8) can be determined from shot noise measurements at low temperatures [8,9].

2.4 Shot noise

Shot noise is generated if the stream of injected particles is partitioned on an electronic beam splitter as illustrated in Figure 2 [59–63]. We first emit particles into one of the input arms using a periodically driven electron source, while the other input channel is grounded, as indicated in the right panel of Figure 2. In this case, the time-averaged cross-correlations of the outgoing currents, $\mathcal{P}_{\text{out}}$, is related to the excess first-order correlation function of the incoming excitations as [64]

$$\frac{\mathcal{P}_{\text{out}}}{\mathcal{P}_0} = -\int\limits_0^{\mathcal{T}_0} dt \int\limits_{-\infty}^{\infty} d\tau \left| v_\mu G^{(1)}(t + \tau; t) \right|^2. \tag{10}$$

Here, the factor $\mathcal{P}_0 = e^2 RT/\mathcal{T}_0$ is given by the electron charge e, the reflection R and transmission probabilities $T = 1 - R$ of the beam splitter, and the period of the drive $\mathcal{T}_0$. To keep the discussion simple, we assume that electrons injected in different periods do not overlap. We can then extend the limits of the integral over t to infinity. Upon substituting equations (5) into (10), combined with equations (3) and (6), we now arrive at an expression for the shot noise in the case $\eta_1 \eta_2 = -1$, which reads

$$\frac{\mathcal{P}_{\text{out}}}{\mathcal{P}_0} = -N = -2\left(1 - |J_-|^2\right). \tag{11}$$

This result shows that the shot noise is given by the product of two factors: one, $-2\mathcal{P}_0$, is the shot noise produced by two independent particles. The other one, $1 - |J_-|^2$, is the probability that the two particles do not annihilate each other.

Note that in the case of electron–electron (or hole–hole) injection, the overlap integral is zero, $J_+ = 0$, and the shot noise, equation (10), is given by the sum of the independent contributions of two particles, $\mathcal{P}_{\text{out}} = -2\mathcal{P}_0$.

2.4.1 Annihilation versus the electronic Hong-Ou-Mandel effect

Equation (11), replacing J_- by J_+, also describes the situation where two electrons (or two holes) are injected into different input arms and interfere at the beam splitter as in a Hong-Ou-Mandel interferometer [6,54,61,65]. Note that we are discussing two-particle, not single-particle, interference in the following. Although the equation is formally the same for the two cases, the physical interpretation of the overlap integral in equation (6) is completely different.

In the *non-local* setup in the left panel of Figure 2, the two sources emit particles into different input channels, and the emitted electrons or holes ($\eta_1\eta_2 = +1$) are initially uncorrelated. They interfere when they arrive at the beam splitter, where the Pauli exclusion principle forces them to exit via different output arms [61]. In this case, the overlap of the wave functions at the beam splitter determines the suppression of the shot noise, and its exact value, $J_+ \neq 0$, can be controlled by adjusting the relative emissions times. On the other hand, if an electron and a hole are injected, $\eta_1\eta_2 = -1$, they scatter on the beam splitter independently, since their energy is different such that the Pauli exclusion principle does not apply, and the overlap integral vanishes, $J_- = 0$.

By contrast, in the *local* setup in the right panel of Figure 2, the two emitters are placed in the same input arm to make up a composite source. In this case, two injected electrons (or holes) with $\eta_1\eta_2 = +1$ interfere already upon emission. The Pauli exclusion principle forces the two injected electrons (or holes) to be in orthogonal quantum states and the overlap must vanish, $J_+ = 0$, independently of the emission times. On the other hand, if one source emits an electron and the other a hole, $\eta_1\eta_2 = -1$, the overlap integral is not necessarily zero, $J_- \neq 0$ and it characterizes correlations between the entire injected state and the vacuum (the untouched Fermi sea) according to equation (9). More precisely, the overlap integral J_- is just the quantum-mechanical amplitude of the annihilation process, in which an electron injected by one source is annihilated by a hole from the other source, such that no particles effectively are emitted towards the beam splitter. Importantly, the value of the overlap integral, $J_- \neq 0$, can in this case be continuously tuned by changing the emission times.

We recall that we here consider zero temperature and refer the reader to references [66,67] for a discussion of electron–hole interference at nonzero temperatures in the non-local setup and to references [68] for a discussion of electron–electron interference at nonzero temperatures in the local setup.

As we have seen, the shot noise suppression is clearly caused by different physical processes. In the non-local setup, the shot noise suppression occurs due to the interference of identical particles at the beam splitter [69–71]. By contrast, for the local setup, the shot noise suppression is due to the decreased number of injected particles, since electron and holes may annihilate each other close to the emitters. Shot noise suppression forms the basis of single-electron state tomography based on Hong-Ou-Mandel interferometry [21], and one may anticipate that similar ideas can be developed based on the annihilation effect for the local setup. Importantly, with the sources placed close to each other as in the right panel of Figure 2, the setup becomes less susceptible to decoherence along the electron waveguide [27,72].

3 Scattering theory of composite two-electron sources

We now describe the scattering theory of composite two-electron sources. To this end, we first consider a single-particle emitter that is attached to a chiral one-dimensional electron waveguide. The source is driven by a classical periodic field with period $\mathcal{T}_0 = 2\pi/\Omega$, for example an electric potential that is applied with a gate electrode.

The effect of a periodic driving field can be described by a Floquet scattering matrix S_{F}, whose elements $S_{\mathrm{F}}(E_n, E)$ are the photon-assisted amplitudes for an electron with energy E to exchange n energy quanta of size $\hbar\Omega$ with the driving field such that its energy becomes $E_n = E + n\hbar\Omega$ [73]. The scattering amplitudes relate the electron operators in second quantization before and after the source, $\hat{a}$ and $\hat{b}$, respectively, as

$$\hat{b}(E_n) = S_{\mathrm{F}}(E_n, E)\,\hat{a}(E) \tag{12}$$

for annihilation operators and

$$\hat{b}^\dagger(E_n) = S_{\mathrm{F}}^*(E_n, E)\,\hat{a}^\dagger(E) \tag{13}$$

for creation operators. The electrons before the source are in equilibrium and are characterized by the Fermi distribution function

$$f(E) = \frac{1}{1 + \exp\left[\frac{E - \mu}{k_B \theta}\right]}, \tag{14}$$

where μ is Fermi energy, the temperature is θ, and k_{B} is the Boltzmann constant. The quantum-mechanical average used in the definition of $G^{(1)}$ describes the fermionic operators before the source, where the particles are in equilibrium and we have

$$\left\langle \hat{a}^\dagger(E)\,\hat{a}(E') \right\rangle = \delta(E - E')\,f(E). \tag{15}$$

In the wide band limit, the excess first-order correlation function then becomes [74]

$$G^{(1)}(t_1; t_2) = \frac{1}{h v_\mu} \int dE f(E)\, e^{\frac{i}{\hbar} E(t_1 - t_2)} \left\{ S_{\mathrm{in}}^*(t_1, E) S_{\mathrm{in}}(t_2, E) - 1 \right\}, \tag{16}$$

where we have introduced the inverse Fourier transform of the Floquet amplitudes [75]

$$S_{\mathrm{in}}(t, E) = \sum_{n=-\infty}^{\infty} e^{-in\Omega t} S_{\mathrm{F}}(E_n, E). \tag{17}$$

These expressions allow us to describe dynamic single-electron emitters.

3.1 Composite sources

We can now describe two-particle sources composed of two single-particle emitters connected in series [45]. If each source separately operates as an ideal single-particle emitter, we can expect that the composite source will work as a two-particle emitter.

We place the two single-particle emitters, each described by the scattering matrices $S_{\mathrm{in}}^{\mathrm{L}}$ and $S_{\mathrm{in}}^{\mathrm{R}}$, in close proximity to form a composite source. To be specific, we

choose S_{in}^{L} to describe first emitter upstream. The total scattering amplitude of the composite source can then be calculated as [57]

$$S_{\text{in}}^{\text{tot}}(t, E) = \sum_{n=-\infty}^{\infty} \int_0^{\mathcal{T}_0} \frac{d\tau}{\mathcal{T}_0} e^{in\Omega(\tau - t)} S_{\text{in}}^{\text{R}}(t, E_n) S_{\text{in}}^{\text{L}}(\tau, E), \tag{18}$$

where we have neglected the distance between the sources. At zero temperature and in the wide band limit, the distance between the emitters can be accounted for simply by adjusting the injection times of the two emitters.

The correlation function of the composite source can be calculated using Eq. (16) by replacing S_{in} with $S_{\text{in}}^{\text{tot}}$. The correlation function then consists of three terms,

$$G_{\text{tot}}^{(1)} = G_{\text{R}}^{(1)} + G_{\text{L}}^{(1)} + \delta G_{\text{LR}}^{(1)}, \tag{19}$$

where $G_j^{(1)}$, $j = $ L, R, is given in equation (16) with S_{in} replaced by S_{in}^j, while the last term accounts for the combined effect of the two single-particle emitters and reads

$$\delta G_{\text{LR}}^{(1)} = \frac{1}{hv_\mu} \int dE f(E) e^{\frac{i}{\hbar}E(t_1 - t_2)} \sum_{m,n} \int\!\!\int_0^{\mathcal{T}_0} \frac{d\tau'}{\mathcal{T}_0} \frac{d\tau}{\mathcal{T}_0} e^{-im\Omega(\tau' - t_1)} e^{in\Omega(\tau - t_2)} \tag{20}$$

$$\times \left\{ \left[S_{\text{in}}^{\text{R}}(t_1, E_m) \right]^* S_{\text{in}}^{\text{R}}(t_2, E_n) - 1 \right\} \left\{ \left[S_{\text{in}}^{\text{L}}(\tau', E) \right]^* S_{\text{in}}^{\text{L}}(\tau, E) - 1 \right\}.$$

With these expressions, we can now describe the composite two-particle sources.

4 Examples

We are now ready to discuss examples of composite two-particle sources. We restrict ourselves to zero temperature, $\theta = 0$, where the Fermi distribution is a step function, $f(E) = \Theta(\mu - E)$, with $\Theta(x)$ being the Heaviside function.

4.1 Adiabatic injection

If the scattering amplitude of each single-particle source, S_{in}^j, is energy-independent, the total amplitude is simply given by the product, $S_{\text{in}}^{\text{tot}}(t) = S_{\text{in}}^{\text{R}}(t) S_{\text{in}}^{\text{L}}(t)$ [45,55]. The expression for the correlation function also greatly simplifies. In particular, at zero temperature, equations (16), (19), and (20) in combination give us

$$G_j^{(1)}(t_1; t_2) = \frac{e^{\frac{i}{\hbar}\mu(t_1 - t_2)}}{v_\mu} \frac{\left[S_{\text{in}}^j(t_1) \right]^* S_{\text{in}}^j(t_2) - 1}{2\pi i (t_1 - t_2)}, \tag{21a}$$

$$G_{\text{tot}}^{(1)}(t_1; t_2) = G_{\text{R}}^{(1)}(t_1; t_2) + \left[S_{\text{in}}^{\text{R}}(t_1) \right]^* G_{\text{L}}^{(1)}(t_1; t_2) S_{\text{in}}^{\text{R}}(t_2). \tag{21b}$$

The last equation admits the following interpretation: the quantum state injected by the composite source is the sum of the quantum state injected by the downstream source and the state injected by the upstream source after being modified by the downstream one. Although this might be a rather artificial interpretation, since we

can't really divide the quantum phase-coherent system into parts, it provides a useful description of what is happening in the system.

Equation (21) tells us that in the adiabatic case, if each source separately works as a single-electron emitter, the two emitters form a perfect two-particle source which excites no unwanted electron-hole pairs. Indeed, if the correlation function of each individual source has the form given in equation (2), $G_j^{(1)}(t_1; t_2) \sim \psi_j^*(t_1)\,\psi_j(t_2)$, $j = $ L, R, the correlation function of the composite source, $G_{\text{tot}}^{(1)}$, is given by equation (5) with, for instance, $\psi_1(t) = \psi_{\text{R}}(t)$ and $\psi_2(t) = S_{\text{in}}^{\text{R}}(t)\,\psi_{\text{L}}(t)$. We note that in the adiabatic limit, the scattering amplitude of an emitter coupled to a chiral one-dimensional channel is just a phase factor, $S_{\text{in}}^j = e^{i\sigma_j}$, so that the modulus is unity, $|S_{\text{in}}^j| = 1$. For this reason, ψ_2 is normalized if ψ_{L} is also normalized. This line of reasoning can be generalized to any number of sources operating in the adiabatic regime [51].

4.2 Levitons

A paradigmatic example of an energy independent source is the case of an AC voltage applied to a metallic contact from which a chiral edge state originates. The scattering amplitude is the phase factor, $S_{\text{in}}(t) = \exp[-i\,(e/\hbar)\int_{-\infty}^t dt'\,V(t')]$, where $V(t)$ is the time-dependent voltage [50]. If the voltage is a sequence of Lorentzian voltage pulses of a definite amplitude [76–86],

$$eV(t) = \eta \sum_{m=-\infty}^{\infty} \frac{2\hbar\Gamma_\tau}{\left(t - \tau - m\mathcal{T}_0\right)^2 + \Gamma_\tau^2}, \tag{22}$$

a sequence of single electrons ($\eta = +1$) or holes ($\eta = -1$) are injected [36–38]. These particles are called *levitons* [8]. The parameter Γ_τ is the half-width of the density profile of the wave packets. It also defines the energy of each leviton, $\mathcal{E} = \hbar/(2\Gamma_\tau)$ [38]. The parameter τ determines the position of the peak of the wave packet within the period, $0 < \tau < \mathcal{T}_0$. In general, when $\mathcal{T}_0 \sim \Gamma_\tau$, the particles injected during different periods are overlapping, the resulting state is thus strictly speaking a multi-particle state, and the corresponding wave functions were analysed in reference [51].

To simplify our analysis of two Lorentzian voltage pulses being applied per period, we consider the limiting case $\mathcal{T}_0 \gg \Gamma_\tau$ and restrict ourselves to a single long period. This approach can also be employed when Floquet scattering theory is used to describe a non-periodic process as we will see in Section 4.3 [53]. The applied voltage is then the sum of two Lorentzian pulses, $V_{\text{tot}} = V_{\text{L}} + V_{\text{R}}$, with

$$eV_j(t) = \eta_j \frac{2\hbar\Gamma_j}{\left(t - \tau_j\right)^2 + \Gamma_j^2}. \tag{23}$$

Here, the time t extends over the full, long period $\mathcal{T}_0 \gg \Gamma_j$. The voltages $V_{\text{L,R}}$ now play the role of single-particle sources, while the total voltage V_{tot} effectively is our composite two-particle source. The corresponding scattering amplitudes read [35]

$$S_{\text{in}}^j(t) = \frac{t - \tau_j + i\eta_j\Gamma_j}{t - \tau_j - i\eta_j\Gamma_j}. \tag{24}$$

According to equation (21), the correlation function of the composite source has the form of equation (5) with $\eta_1 = \eta_R$, $\eta_2 = \eta_L$ and the following wave functions [40,50]

$$\psi_1(t) = \frac{\sqrt{\Gamma_R/\pi}}{t - \tau_R - i\eta_R\Gamma_R}, \quad \psi_2(t) = \frac{\sqrt{\Gamma_L/\pi}}{t - \tau_L - i\eta_L\Gamma_L} \frac{t - \tau_R + i\eta_R\Gamma_R}{t - \tau_R - i\eta_R\Gamma_R}, \tag{25}$$

which are normalized according to equation (3). When both voltages have the same sign, $\eta_L = \eta_R$, the overlap integral in equation (6) is zero, $J_+ = 0$, recalling that the subscript stands for the sign of the product $\eta_L\eta_R$. In other words, when both voltages excite particles with the same charge (two electrons or two holes), the particles occupy orthogonal states in accordance with the Pauli exclusion principle.

By contrast, if the two voltages V_L and V_R excite particles of opposite charge, $\eta_L = -\eta_R$, the overlap integral is non-zero, and one may interpret this as the particle generated by one source being annihilated by the other with probability $|J_-|^2$. Indeed, using equations (6), (8), and (25), the number of emitted particles reads [38]

$$N = 2\left(1 - |J_-|^2\right) \le 2, \quad |J_-|^2 = \frac{4\Gamma_L\Gamma_R}{\tau^2 + (\Gamma_L + \Gamma_R)^2}, \tag{26}$$

where $\tau = \tau_L - \tau_R$ is the time difference between the two voltage pulses. If the electron and hole wave packets have the same width, $\Gamma_L = \Gamma_R$, and are injected simultaneously, $\tau = 0$, the annihilation is complete and no particles are emitted, $N = 0$ [45]. For this reason, we can refer to a hole-like leviton as an *anti-leviton*, and we see how a leviton created by one voltage pulse and a hole created by another voltage pulse can completely annihilate each other. Of course, in this simple case, the voltage pulses simply cancel each other, such that the total applied voltage vanishes.

Interestingly, the overlap integral in equation (26) has the same time dependence as the wave function squared in equation (25), however, with both the amplitude and the width of the wave packet being renormalized. This fact can be used to access the time-dependent density profile of a single-electron wave packet via a time-averaging measurement like the shot noise measurement described by equation (11).

4.3 Non-adiabatic injection

We now move on to non-adiabatic particle injection. Theory predicts that an electron and a hole injected in an irreversible decay process do not annihilate each other [57]. Therefore, one may speculate that complete annihilation only occurs in the adiabatic regime. To support this expectation, we now discuss a single-particle source that can be tuned from the adiabatic to the non-adiabatic regime. Specifically, we consider single-particle emission into a Fermi sea from a single quantum level that can be varied linearly in time with rapidity c. The corresponding scattering amplitude reads [35]

$$S_{\text{in}}(t, E) = 1 - 2\int_0^\infty d\xi e^{-\xi} e^{-i\frac{t-\tau}{\Gamma_\tau}\xi} e^{i\zeta\xi^2} e^{i\zeta\frac{E-\mu}{\bar{\varepsilon}}\xi}, \tag{27}$$

where τ is the time when the quantum level would cross the Fermi energy μ, if there were no coupling. The width of the injected wave packet due to the coupling to the Fermi sea is denoted by Γ_τ. This width determines the time window during which the broadened quantum-dot level crosses the Fermi level. The coupling strength can also be characterized by the dwell time, τ_D, which is the time it takes an electron to decay from the quantum level at a fixed energy above the Fermi level. In addition,

the crossing time Γ_τ depends on the rapidity c. Thus, the parameter that enters equation (27) is defined as $\Gamma_\tau = \hbar/(2c\tau_D)$. Moreover, the parameter ζ is given by the ratio of the two characteristic time scales, $\zeta = \tau_D/\Gamma_\tau$, and it controls how adiabatic the driving is. Specifically, with $\zeta = 0$, we recover the adiabatic solution in equation (24). Finally, $\mathcal{E} = \hbar/(2\Gamma_\tau)$ is the energy of the injected particle relative to the Fermi level [64].

The wave function of the injected particle reads $\Psi(t) = e^{-\frac{i}{\hbar}\mu t}\psi(t)$ with [35]

$$\psi(t) = \frac{1}{\sqrt{\pi |\Gamma_\tau|}} \int\limits_0^\infty d\xi \, e^{-\xi} e^{-i\frac{t-\tau}{\Gamma_\tau}\xi} e^{i\zeta\xi^2}. \tag{28}$$

The wave function is normalized according to equation (3), and we note that the two parameters Γ_τ and ζ both depend on the rapidity c. If the rapidity is positive (negative), $c > 0$ ($c < 0$), an electron (hole) is injected. To take this into account, we use $\eta\Gamma_\tau$ and $\eta\zeta$, with both Γ_τ and ζ being positive, and $\eta = 1(-1)$ for electron (hole) injection.

4.3.1 Two-particle injection

We now take two quantum dot levels as above and attach them in series to a chiral waveguide. As before, we use the subscript L for the upstream source and R for the downstream source. The scattering amplitude of each source reads

$$S_{\text{in}}^j(t, E) = 1 - 2\int\limits_0^\infty d\xi \, e^{-\xi} e^{-i\eta_j\frac{t-\tau_j}{\Gamma_j}\xi} e^{i\eta_j\zeta_j\xi^2} e^{i\zeta_j\frac{E-\mu}{\mathcal{E}_j}\xi}, \quad j = \text{L, R}, \tag{29}$$

where the last exponential factor does not contain η_j, since the ratio $\zeta_j/\mathcal{E}_j$ is the same for electron ($\eta_j = 1$) and hole ($\eta_j = -1$) injection.
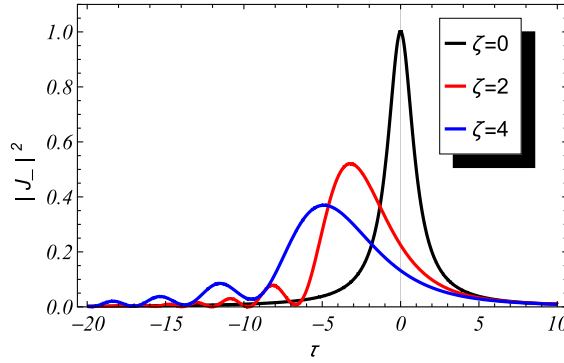
Based on this expression, we can calculate the scattering amplitude of the composite source $S_{\text{in}}^{\text{tot}}$ using equation (18) and, furthermore, the correlation function $G_{\text{tot}}^{(1)}$ using equation (16). The calculation is in principle straightforward, however, it is rather lengthy, and the details are presented in Appendix A of the Supplementary Material.

At zero temperature, the result has the form of equation (5) with $\eta_1 = \eta_R$ and $\psi_1(t) = \psi_R(t)$, where ψ_R is the wave function of a particle that would be injected by the downstream source on its own,

$$\psi_R(t) = \frac{1}{\sqrt{\pi\Gamma_R}} \int\limits_0^\infty d\xi \, e^{-\xi} e^{-i\eta_R\frac{t-\tau_R}{\Gamma_R}\xi} e^{i\eta_R\zeta_R\xi^2}. \tag{30}$$

For the second contribution in equation (5), we have $\eta_2 = \eta_L$ and the wave function

$$\psi_2(t) = \frac{1}{\sqrt{\pi\Gamma_L}} \int\limits_0^\infty d\xi \, e^{-\xi} e^{-i\eta_L\frac{t-\tau_L}{\Gamma_L}\xi} e^{i\eta_L\zeta_L\xi^2}$$

$$\times \left\{ 1 - 2\int\limits_0^\infty d\chi \, e^{-\chi} e^{-i\eta_R\frac{t-\tau_R}{\Gamma_R}\chi} e^{i\eta_R\zeta_R\chi^2} e^{i\eta_L\zeta_R\frac{\Gamma_R}{\Gamma_L}2\xi\chi} \right\}. \tag{31}$$

Fig. 3. The overlap integral $|J_-|^2$ in equation (32) as a function of the scaled time delay $\tau \equiv \bar{t}$ for the renormalized non-adiabaticity parameter $\zeta \equiv \bar{\zeta} = 0, 2, 4$. The overlap integral is given in units of $2\sqrt{\Gamma_R \Gamma_L}/(\Gamma_R + \Gamma_L)$.

The wave function is normalized as shown in Appendix B of the Supplementary Material. Note that the equation above consists of two distinct terms, $\psi_2 = \psi_L + \delta\psi_{LR}$, as compared to equations (19) and (20). First, ψ_L is given by equation (30) with the subscript R replaced by L, i.e., it represents a particle injected upstream in the absence of a downstream source. Second, $\delta\psi_{LR}$ describes the joint effect of the two sources. The term $\delta\psi_{LR}$ is important, because it is responsible for the orthogonalization of ψ_1 and ψ_2 if $\eta_L\eta_R = +1$ and for the annihilation effect if $\eta_L\eta_R = -1$.

It is easy to show that the two wave functions are orthogonal, if $\eta_L = \eta_R$. In other words, the overlap integral in equation (6) vanishes, $J_+ = 0$, with the subscript referring to the sign of the product $\eta_L\eta_R$. The details of these calculations are presented in Appendix C of the Supplementary Material. Hence, if the sources emit particles of the same kind, electrons or holes, the resulting two-particle state contains particles in orthogonal states as required by the Pauli exclusion principle. By contrast, if $\eta_L = -\eta_R$, the two wave functions are no longer orthogonal (see Appendix D of the Supplementary Material for further details), and we have

$$J_-\left(\bar{t}\right) = \frac{2\sqrt{\Gamma_R\Gamma_L}}{\Gamma_R + \Gamma_L} \int\limits_0^\infty d\xi e^{-\xi} e^{i\bar{t}\xi} e^{i\bar{\zeta}\xi^2}, \; \bar{t} = \frac{\eta_R\tau_R + \eta_L\tau_L}{\Gamma_R + \Gamma_L}, \; \bar{\zeta} = \eta_L \frac{\Gamma_R^2\zeta_R + \Gamma_L^2\zeta_L}{(\Gamma_R + \Gamma_L)^2}. \quad (32)$$

As already discussed, a nonzero overlap integral, $J_- \neq 0$, indicates that the particles partially annihilate each other according to equations (8) and (26), and the degree of annihilation, $|J_-|^2$, can be accessed through shot noise measurements as shown in equation (11). We note that for adiabatic injection, $\zeta_L = \zeta_R = 0$, equation (32) agrees with equation (26).

Similar to the case of leviton injection in equation (26) and the subsequent discussion, the overlap integral $J_-\left(-\bar{t}\right)$ in equation (32) has the form of the wave function of a single emitter, but with the renormalized nonadiabaticity parameter $\zeta \to \bar{\zeta}$, cf. $\psi\left([t - \tau]/\Gamma_\tau\right)$ in equation (28). Therefore, for a composite source consisting of two identical emitters, one can experimentally access the time-dependent electron density profile injected by a single-particle source by measuring the probability of annihilation as a function of the time delay between the emitters.

In Figure 3, we show the overlap $|J_-|^2$ as a function of the time delay between particle emissions for different values of the non-adiabaticity parameter. The maximum annihilation takes place in the case of adiabatic injection, $\zeta_L = \zeta_R = 0$ (black line). In this case, a zero time delay ($\tau = 0$) leads to the transfer of an electron

from one source to the other. Beyond the adiabatic regime, an increase in the rapidity suppresses the degree of annihilation at the maximum, and also it increases the asymmetry of the peaks. This behavior is in full agreement with a similar modification of the single-electron wave functions found in reference [35]. The wavy structure on the left slope is a manifestation of quantum-mechanical interference *in time* that occurs during tunneling from a quantum level, whose position changes with time [53]. An experimental observation of such a delicate quantum effect would be an important step towards the development of a time-resolved detector of single- and few-electron quantum states.

5 Conclusions

We have presented a Floquet scattering theory of composite two-particle sources composed of several single-particle emitters connected in series to a chiral waveguide. The setup can include more than two single-particle emitters, and the individual emitters may be of different types. For example, the combination of a leviton source with a quantum capacitor is within experimental reach, and it would enable the use of one source to characterize the other [84].

Using our theory, we have analysed several situations where ideal two-particle injection can be achieved. In particular, we have considered adiabatic injection using emitters with an energy-independent scattering amplitude. If both single-particle emitters operate under ideal conditions, the composite source emits exactly two particles without exciting any unwanted electron-hole pairs. An example of such an emitter is provided by a leviton source.

Going beyond the adiabatic regime, we have analysed a setup with two quantum levels that are shifted with a constant rapidity across the Fermi level of the external reservoir. This setup enables perfect two-particle injection both for adiabatic and non-adiabatic working conditions, where the injected wave packets have symmetric and asymmetric density profiles, respectively.

As an interesting new application of composite two-particle sources, we have examined the regime where one source injects an electron and the other a hole. In this case, the electron and the hole may annihilate each other, effectively meaning that one source reabsorbs the particle that was emitted by the other. If the probability of annihilation is less than one, a superposition of a two-fermion state and the vacuum state is formed. The amplitude of the annihilation process is given by the overlap of the injected single-particle quantum states. This fact can be used to develop single-electron tomography protocols based on this reabsorption effect. The advantage of our approach lies in the compactness of the setup, which helps avoiding decoherence, which is a major problem for quantum coherent electronics.

Author contribution statement

M.M., J.K., P.B. and C.F. contributed to the formulation of the problem and implementation of the research, to the analysis of the results and to the writing of the manuscript.

References

1. C. Bäuerle, D.C. Glattli, T. Meunier, F. Portier, P. Roche, P. Roulleau, S. Takada, X. Waintal, Rep. Prog. Phys. **81**, 056503 (2018)
2. J. Splettstoesser, R.J. Haug, Phys. Status Solidi B **254**, 1770217 (2017)
3. J.P. Pekola, O.P. Saira, V.F. Maisi, A. Kemppinen, M. Mottönen, Y.A. Pashkin, D.V. Averin, Rev. Mod. Phys. **85**, 1421 (2013)
4. S.P. Giblin, A. Fujiwara, G. Yamahata, M.H. Bae, N. Kim, A. Rossi, M. Mottönen, M. Kataoka (2019), arXiv:1901.05218v1
5. J. Splettstoesser, M. Moskalets, M. Büttiker, Phys. Rev. Lett. **103**, 076804 (2009)
6. E. Bocquillon et al., Ann. Phys. **526**, 1 (2014)
7. R. Hanbury Brown, R.Q. Twiss, Nature **178**, 1046 (1956)
8. J. Dubois, T. Jullien, F. Portier, P. Roche, A. Cavanna, Y. Jin, W. Wegscheider, P. Roulleau, D.C. Glattli, Nature **502**, 659 (2013)
9. E. Bocquillon, F.D. Parmentier, C. Grenier, J.M. Berroir, P. Degiovanni, D.C. Glattli, B. Plaçais, A. Cavanna, Y. Jin, G. Fève, Phys. Rev. Lett. **108**, 196803 (2012)
10. D.C. Glattli, P. Roulleau, Phys. Rev. B **97**, 125407 (2018)
11. M. Henny, S. Oberholzer, C. Strunk, T. Heinzel, K. Ensslin, M. Holland, C. Schönenberger, Science **284**, 296 (1999)
12. W.D. Oliver, J. Kim, R.C. Liu, Y. Yamamoto, Science **284**, 299 (1999)
13. S. Oberholzer, M. Henny, C. Strunk, C. Schönenberger, T. Heinzel, K. Ensslin, M. Holland, Physica E **6**, 314 (2000)
14. I. Neder, N. Ofek, Y. Chung, M. Heiblum, D. Mahalu, V. Umansky, Nature **448**, 333 (2007)
15. C.K. Hong, Z.Y. Ou, L. Mandel, Phys. Rev. Lett. **59**, 2044 (1987)
16. V. Freulon, A. Marguerite, J.M. Berroir, B. Plaçais, A. Cavanna, Y. Jin, G. Fève, Nat. Commun. **6**, 6854 (2015)
17. E. Bocquillon, V. Freulon, J.M. Berroir, P. Degiovanni, B. Plaçais, A. Cavanna, Y. Jin, G. Fève, Science **339**, 1054 (2013)
18. A. Marguerite, E. Bocquillon, J.M. Berroir, B. Plaçais, A. Cavanna, Y. Jin, P. Degiovanni, G. Fève, Phys. Status Solidi B **254**, 1600618 (2016)
19. D.C. Glattli, P.S. Roulleau, Phys. Status Solidi B **254**, 1600650 (2016)
20. A. Marguerite et al., Phys. Rev. B **94**, 115311 (2016)
21. C. Grenier, R. Hervé, E. Bocquillon, F.D. Parmentier, B. Plaçais, J.M. Berroir, G. Fève, P. Degiovanni, New J. Phys. **13**, 093007 (2011)
22. T. Jullien, P. Roulleau, B. Roche, A. Cavanna, Y. Jin, D.C. Glattli, Nature **514**, 603 (2014)
23. A. Marguerite et al. (2017), arXiv:1710.11181v1
24. J.D. Fletcher, N. Johnson, E. Locane, P. See, J.P. Griffiths, I. Farrer, D.A. Ritchie, P.W. Brouwer, V. Kashcheyevs, M. Kataoka, Nature communications **10**, 5298 (2019)
25. C. Altimiras, H. le Sueur, U. Gennser, A. Cavanna, D. Mailly, F. Pierre, Phys. Rev. Lett. **105**, 226804 (2010)
26. P.A. Huynh, F. Portier, H. le Sueur, G. Faini, U. Gennser, D. Mailly, F. Pierre, W. Wegscheider, P. Roche, Phys. Rev. Lett. **108**, 256802 (2012)
27. C. Cabart, B. Roussel, G. Fève, P. Degiovanni, Phys. Rev. B **98**, 155302 (2018)
28. R.H. Rodriguez, F.D. Parmentier, P. Roulleau, U. Gennser, A. Cavanna, F. Portier, D. Mailly, P. Roche (2019), arXiv:1903.05919v1
29. H. Duprez, E. Sivre, A. Anthore, A. Aassime, A. Cavanna, A. Ouerghi, U. Gennser, F. Pierre, Phys Rev X **9**, 021030 (2019)
30. M. Kataoka, N. Johnson, C. Emary, P. See, J.P. Griffiths, G.A.C. Jones, I. Farrer, D.A. Ritchie, M. Pepper, T.J.B.M. Janssen, Phys. Rev. Lett. **116**, 126803 (2016)
31. N. Johnson et al., Phys. Rev. Lett. **121**, 137703 (2018)
32. G. Fève, A. Mahé, J.M. Berroir, T. Kontos, B. Plaçais, D.C. Glattli, A. Cavanna, B. Etienne, Y. Jin, Science **316**, 1169 (2007)
33. J. Gabelli, G. Fève, J.M. Berroir, B. Plaçais, A. Cavanna, B. Etienne, Y. Jin, Science **313**, 499 (2006)

34. M. Büttiker, H. Thomas, A. Prêtre, Phys. Lett. A **180**, 364 (1993)
35. J. Keeling, A.V. Shytov, L.S. Levitov, Phys. Rev. Lett. **101**, 196404 (2008)
36. L.S. Levitov, H. Lee, G.B. Lesovik, J. Math. Phys. **37**, 4845 (1996)
37. D.A. Ivanov, H.W. Lee, L.S. Levitov, Phys. Rev. B **56**, 6839 (1997)
38. J. Keeling, I. Klich, L.S. Levitov, Phys. Rev. Lett. **97**, 116403 (2006)
39. M. Misiorny, G. Fève, J. Splettstoesser, Phys. Rev. B **97**, 075426 (2018)
40. D.C. Glattli, P. Roulleau, Physica E **76**, 216 (2016)
41. J. Waldie, P. See, V. Kashcheyevs, J.P. Griffiths, I. Farrer, G.A.C. Jones, D.A. Ritchie, T.J.B.M. Janssen, M. Kataoka, Phys. Rev. B **92**, 125305 (2015)
42. N. Ubbelohde, F. Hohls, V. Kashcheyevs, T. Wagner, L. Fricke, B. Kästner, K. Pierz, H.W. Schumacher, R.J. Haug, Nat. Nanotechnol. **10**, 46 (2014)
43. J.D. Fletcher et al., Phys. Rev. Lett. **111**, 216807 (2013)
44. L. Fricke et al., Phys. Rev. Lett. **110**, 126803 (2013)
45. J. Splettstoesser, S. Ol'khovskaya, M. Moskalets, M. Büttiker, Phys. Rev. B **78**, 205110 (2008)
46. D. Litinski, P. Brouwer, M. Filippone, Phys. Rev. B **96**, 085429 (2017)
47. G. Wagner, D.X. Nguyen, D.L. Kovrizhin, S.H. Simon, Phys. Rev. Lett. **122**, 127701 (2019)
48. C. Grenier, R. Hervé, G. Fève, P. Degiovanni, Mod. Phys. Lett. B **25**, 1053 (2011)
49. B. Roussel, C. Cabart, G. Fève, E. Thibierge, P. Degiovanni, Phys. Status Solidi B **254**, 1600621 (2017)
50. C. Grenier, J. Dubois, T. Jullien, P. Roulleau, D.C. Glattli, P. Degiovanni, Phys. Rev. B **88**, 085302 (2013)
51. M. Moskalets, Phys. Rev. B **91**, 195431 (2015)
52. M. Moskalets, G. Haack, Physica E **75**, 358 (2016)
53. M. Moskalets, Low Temp. Phys. **43**, 865 (2017)
54. M. Moskalets, Phys. Rev. B **96**, 165423 (2017)
55. M. Moskalets, Phys. Rev. B **89**, 045402 (2014)
56. M. Moskalets, M. Büttiker, Phys. Rev. B **80**, 081302(R) (2009)
57. M. Moskalets, G. Haack, M. Büttiker, Phys. Rev. B **87**, 125429 (2013)
58. S. Juergens, J. Splettstoesser, M. Moskalets, Europhys. Lett. **96**, 37011 (2011)
59. W. Schottky, Ann. Phys. **362**, 541 (1918)
60. M. Reznikov, R. de Picciotto, M. Heiblum, D.C. Glattli, A. Kumar, L. Saminadayar, Superlattice Microst. **23**, 901 (1998)
61. Ya. Blanter, M. Büttiker, Phys. Rep. **336**, 1 (2000)
62. M. Büttiker, Phys. Rev. B **46**, 12485 (1992)
63. R. Liu, B. Odom, Y. Yamamoto, S. Tarucha, Nature **391**, 263 (1998)
64. M. Moskalets, G. Haack, Phys. Status Solidi B **254**, 1600616 (2016)
65. D. Ferraro, F. Ronetti, L. Vannucci, M. Acciai, J. Rech, T. Jockheere, T. Martin, M. Sassetti, Eur. Phys. J. Special Topics **227**, 1345 (2018)
66. T. Jonckheere, J. Rech, C. Wahl, T. Martin, Phys. Rev. B **86**, 125425 (2012)
67. J. Rech, C. Wahl, T. Jonckheere, T. Martin, J. Stat. Mech.: Theory Exp. **2016**, 054008 (2016)
68. M. Moskalets, Phys. Rev. B **97**, 155411 (2018)
69. S. Ol'khovskaya, J. Splettstoesser, M. Moskalets, M. Büttiker, Phys. Rev. Lett. **101**, 166802 (2008)
70. G. Fève, P. Degiovanni, T. Jolicoeur, Phys. Rev. B **77**, 035308 (2008)
71. M. Moskalets, M. Büttiker, Phys. Rev. B **83**, 035316 (2011)
72. E. Iyoda, T. Kato, K. Koshino, T. Martin, Phys. Rev. B **89**, 205318 (2014)
73. M. Moskalets, M. Büttiker, Phys. Rev. B **66**, 205320 (2002)
74. G. Haack, M. Moskalets, M. Büttiker, Phys. Rev. B **87**, 201302 (2013)
75. M. Moskalets, M. Büttiker, Phys. Rev. B **78**, 035301 (12) (2008)
76. J. Dubois, T. Jullien, C. Grenier, P. Degiovanni, P. Roulleau, D.C. Glattli, Phys. Rev. B **88**, 085301 (2013)
77. B. Gaury, X. Waintal, Nat. Commun. **5**, 3844 (2014)
78. D. Dasenbrook, C. Flindt, M. Büttiker, Phys. Rev. Lett. **112**, 146801 (2014)

79. W. Belzig, M. Vanević, Physica E **75**, 22 (2016)
80. J. Rech, D. Ferraro, T. Jonckheere, L. Vannucci, M. Sassetti, T. Martin, Phys. Rev. Lett. **118**, 076801 (2017)
81. T.J. Suzuki, Phys. Rev. B **95**, 241302 (2017)
82. F. Ronetti, L. Vannucci, D. Ferraro, T. Jonckheere, J. Rech, T. Martin, M. Sassetti, Phys. Rev. B **98**, 075401 (2018)
83. I. Safi, Phys. Rev. B **99**, 045101 (2019)
84. P. Burset, J. Kotilahti, M. Moskalets, C. Flindt, Adv. Quantum Technol. **2**, 1970023 (2019)
85. N. Dashti, M. Misiorny, S. Kheradsoud, P. Samuelsson, J. Splettstoesser, Phys. Rev. B **100**, 035405 (2019),
86. D. Ferraro, A. Feller, A. Ghibaudo, E. Thibierge, E. Bocquillon, G. Fève, C. Grenier, P. Degiovanni, Phys. Rev. B **88**, 205303 (2013)